J. Fluid Mech. (1980), *vol.* 97, *part* 3, *pp.* 435–454
Printed in Great Britain

On nose separation

By TUNCER CEBECI, A. K. KHATTAB
Aerodynamics Research Department, Douglas Aircraft Company, Long Beach, California 90846
AND KEITH STEWARTSON
Department of Mathematics, University College, London, England

(Received 29 January 1979)

When solving for three-dimensional laminar and turbulent boundary layers on smooth bodies of revolution at incidence, one has to contend with a difficulty near the nose where the usual formulations of the governing equations are singular. A transformation of the co-ordinate system is described which removes this singularity and enables the solution to be carried smoothly around the nose. A further difficulty arises if the body is slender and it is also shown how this may be overcome. As part of our continuing studies of this problem for both laminar and turbulent flows, we compute the laminar boundary layers on the line of symmetry for thin bodies taking the prolate spheroid as a paradigm. We show that if the angle of incidence α is less than 41°, separation never occurs at the nose no matter how thin the body. In contrast, the value of α which provokes separation at the leading edge of a two-dimensional airfoil tends to zero with the thickness ratio of the airfoil.

1. Introduction

This paper describes one phase of the work done towards the development of a general boundary-layer method for calculating three-dimensional boundary layers on bodies of revolution at incidence. In this paper we address ourselves to the problem of computing boundary layers near the nose region and with the onset of leading-edge separation; this is important for the calculation of transition by stability theory and for the prediction of downstream flow properties including possible separation.

It is well known that separation bubbles can develop near the forward stagnation point of a thin, two-dimensional, plane airfoil at quite small incidences. This phenomenon was first described by Jones (1934) and later Gault (1955) carried out an extensive experimental study. Once separation occurs, some new features of the flow occur, including long and short bubbles, transition to turbulence and bursting. A review of the developments has been written by Tani (1964) and later Gaster (1966) reinforced Gault's conclusion that when separation takes place a noticeable interaction occurs between the boundary layer and the mainstream. The theoretical treatment of the interaction is of special interest to aerodynamicists and an important contribution has been made by Briley & McDonald (1955) who interacted the boundary-layer and inviscid equations over the majority of the flow field but used the full Navier–Stokes equations in the neighbourhood of separation. By these means they were able to avoid the Goldstein (1948) singularity which is an inevitable feature of

0022–1120/80/4426–8750 $02.00

classical boundary-layer theory at separation when the pressure gradient is prescribed. We are interested, in this paper, in the problem of leading-edge separation from the rational standpoint of an asymptotic expansion of the solution of the Navier–Stokes equation in descending powers of the Reynolds number in which it seems likely that the angle of incidence, that just provokes separation, tends to zero with the thickness ratio t of the airfoil. Further, it appears that while the boundary-layer assumption remains true so long as separation does not occur, once it does, the singularity inevitably appears. The correct limiting solution, as the Reynolds number based on the leading-edge radius lead to infinity, is then of a different form and most likely given by the Kirchhoff–Sychev theory, see Smith (1977, 1979), in which a free streamline springs from the airfoil at the maximum slip-velocity on the airfoil and may never reattach. The present study is concerned mainly with determining the boundary-layer properties when separation does not occur and to finding the critical angle of incidence which just provokes separation.

The corresponding problem for bodies of revolution has received less attention but there have been a number of important studies by Wang on the laminar boundary layers on prolate bodies of revolution which have an important bearing and to which we shall refer in detail throughout this paper. The results of his researches are summarized in a recent review, Wang (1976). For example, he has shown (Wang 1970, 1975), that, for the thickness ratio $t = \frac{1}{4}$, separation on the leeside of the line of symmetry occurs near the rear of the body for angles of incidence $\alpha < 40°$ but that at larger values of α a new separation develops very near the nose. The reason is essentially similar to that for two-dimensional flows, it is due to the high curvature of the nose. There is a local velocity overshoot followed immediately afterwards by a short adverse pressure gradient as the main stream returns to a value approximately equal to that at an infinite distance upstream. If this gradient is insufficient to provoke separation, then the boundary layer continues to develop smoothly until, near the rear stagnation point, it encounters a sufficiently severe gradient to compel it to separate. Otherwise the boundary layer breaks down near the nose and as in two dimensions no further progress appears to be possible on a rational theory. It may well be that a free-stream surface then springs off the body but there is much less certainty than in two dimensions about the flow properties once classical theory breaks down.

The remainder of the present paper has been prepared in five sections. The equations appropriate to general prolate spheroids are considered in the following section and those for thin prolate spheroids in § 3: a co-ordinate system appropriate to the nose region and transformations appropriate to the line of symmetry are considered in subsections of § 2. In this paper particular attention is devoted to the 'line of symmetry' equations for the finite and zero-thickness cases. Results are presented in § 4 which also includes parallel results for thin two-dimensional airfoils. The paper concludes with a comparative discussion in § 5.

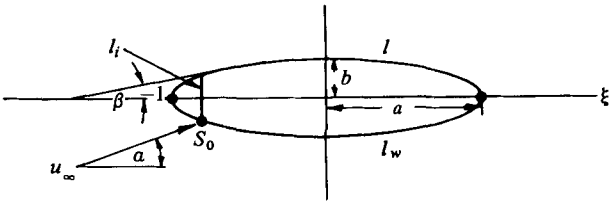

FIGURE 1. Notation for prolate spheroid at incidence.

2. Formulation for prolate spheroids

2.1. *Basic equations*

For a prolate spheroid at incidence (see figure 1), the governing boundary-layer equations for an incompressible laminar flow in a curvilinear orthogonal co-ordinate system are given by the following equations:

$$\textit{Continuity} \quad \frac{\partial}{\partial x}(h_2 u)+\frac{\partial}{\partial \theta}(h_1 w)+\frac{\partial}{\partial y}(h_1 h_2 v) = 0; \tag{1}$$

$$x\textit{ momentum} \quad \frac{u}{h_1}\frac{\partial u}{\partial x}+\frac{w}{h_2}\frac{\partial u}{\partial \theta}+v\frac{\partial u}{\partial y}+w^2 K_2 = -\frac{1}{\rho h_1}\frac{\partial p}{\partial x}+\nu\frac{\partial^2 u}{\partial y^2}; \tag{2}$$

$$\theta\textit{ momentum} \quad \frac{u}{h_1}\frac{\partial w}{\partial x}+\frac{w}{h_2}\frac{\partial w}{\partial \theta}+v\frac{\partial w}{\partial y}-uwK_2 = -\frac{1}{\rho h_2}\frac{\partial p}{\partial \theta}+\nu\frac{\partial^2 w}{\partial y^2}. \tag{3}$$

Here h_1, h_2 are metric coefficients defined by

$$h_1 = \left[\frac{1+\xi^2(t^2-1)}{1-\xi^2}\right]^{\frac{1}{2}}, \quad h_2 = t(1-\xi^2)^{\frac{1}{2}}, \tag{4}$$

where t denotes the thickness ratio ($=b/a$) of the elliptic profile. The parameter K_2/a is the geodesic curvature of the surface lines $\xi(=x/a)$ = const. and is given by

$$K_2 = \frac{t\xi}{h_1 h_2(1-\xi^2)^{\frac{1}{2}}}. \tag{5}$$

The solution of the system (1) to (5) requires boundary conditions and initial conditions. The boundary conditions are:

$$y = 0, \quad u = v = w = 0;$$

$$y \to \infty, \quad u \to u_e(x,\theta), \quad w \to w_e(x,\theta). \tag{6}$$

The velocity components u_e and w_e can be obtained from inviscid theory, (Hirsh & Cebeci 1977), being given by

$$\frac{u_e}{u_{\text{ref}}} = V_0(t)\cos\alpha\cos\beta - V_{90}(t)\sin\alpha\sin\beta\cos\theta, \tag{7a}$$

$$\frac{w_e}{u_{\text{ref}}} = V_{90}(t)\sin\alpha\sin\theta. \tag{7b}$$

Here β denotes the angle between the line tangent to the elliptic profile and the positive ξ axis and given by

$$\cos\beta = \frac{(1-\xi^2)^{\frac{1}{2}}}{[1+\xi^2(t^2-1)]^{\frac{1}{2}}}. \tag{8}$$

The parameters $V_0(t)$ and $V_{90}(t)$ are functions of t, defined by

$$V_0(t) = \frac{(1-t^2)^{\frac{3}{2}}}{(1-t^2)^{\frac{1}{2}} - \frac{1}{2}t^2 \ln\{[1+(1-t^2)^{\frac{1}{2}}]/[1-(1-t^2)^{\frac{1}{2}}]\}}, \tag{9a}$$

$$V_{90}(t) = \frac{2V_0(t)}{2V_0(t)-1}. \tag{9b}$$

The initial conditions in the longitudinal direction can be calculated by takirg advantage of the symmetry conditions. Noting that the circumferential velocity in the boundary layer and the circumferential pressure gradient are identically zero on the line of symmetry, we differentiate this equation with respect to θ to obtain the so-called *attachment-line equations* in the longitudinal direction:

$$\frac{\partial}{\partial x}(h_2 u) + h_1 w_\theta + \frac{\partial}{\partial y}(h_1 h_2 v) = 0; \tag{10}$$

$$\frac{u}{h_1}\frac{\partial u}{\partial x} + v\frac{\partial u}{\partial y} = -\frac{1}{\rho h_1}\frac{\partial p}{\partial x} + \nu\frac{\partial^2 u}{\partial y^2}; \tag{11}$$

$$\frac{u}{h_1}\frac{\partial w_\theta}{\partial x} + \frac{w_\theta^2}{h_2} + v\frac{\partial w_\theta}{\partial y} - uw_\theta K_2 = -\frac{1}{\rho h_2}\frac{\partial^2 p}{\partial \theta^2} + \nu\frac{\partial^2 w_\theta}{\partial y^2}, \tag{12}$$

where $w_\theta = \partial w/\partial\theta$. These equations are subject to the boundary conditions:

$$y = 0, \quad u, v, w = 0; \quad y \to \infty, \quad u \to u_e, \quad w_\theta \to w_{\theta e}. \tag{13}$$

The specification of the initial conditions in the circumferential direction is not quite so easy when body-oriented co-ordinates are used because of the singularity in the properties of h_1, h_2 and K_2 at the nose ($\xi = -1$). A common approach used to circumvent this unpleasant geometric singularity is to revert to an approximate procedure by first performing the integration along the line of symmetry from the stagnation point as near to the nose as possible, then jumping around the body along the line l_i to the same value of x on the leeward side ($\theta = \pi$) as shown in figure 1. Afterwards, the solution may be extended to more general points on the body. Such a procedure, while effective at moderate values of α and/or t leads to difficulties and to inaccuracies as α increases and $t \to 0$. These difficulties can be overcome as described in §§ 2.2 and 3.

An alternative procedure is to use a co-ordinate system on the body surface based on the streamlines of the external flow. The possibilities were explored by Cebeci *et al.* (1973) who noted that a new system would be needed for each value of α and if the fluid is compressible for each Mach number. Further the generation of the co-ordinate lines is very difficult near the nose and the stagnation solution of the boundary-layer equations become singular in these co-ordinates. They abandoned the method but later Geissler (1974) reported some successful computations including a portion of the separation line at $\alpha = 15°$.

2.2. *Nose region co-ordinates*

The difficulties and inaccuracies associated with generating initial conditions in the circumferential direction caused by the singularities in h_1, h_2 and K_2 at $\xi = -1$ can be avoided by using a suitable transformation in the vicinity of the nose. We define new velocity components U, W, V by

$$u = U\cos\theta + W\sin\theta, \tag{14a}$$

$$w = W\cos\theta - U\sin\theta, \quad v = V/ta, \tag{14b}$$

and new co-ordinates X, Y, Z by

$$X = S\cos\theta, \quad Z = S\sin\theta, \quad Y = y/t. \tag{15}$$

Here S is a parameter, which is a function of ξ only, and defined in (20) below.

The purpose of the above transformation is to convert the polar form of equations (1) to (3) near the nose into a quasi-rectangular Cartesian form which is free of singularities. The basic reasoning behind this transformation can be appreciated by noting the advantages of solving the Laplacian near the origin in the form $\partial^2/\partial x^2 + \partial^2/\partial y^2$ compared with $\partial^2/\partial r^2 + (1/r)\,\partial/\partial r + (1/r^2)\,\partial^2/\partial\theta^2$. By means of this transformation it can be shown, after considerable algebra, that equations (1) to (3) reduce to

$$N\left(\frac{\partial U}{\partial X} + \frac{\partial W}{\partial Z}\right) + \frac{\partial V}{\partial Y} - L(UX + WZ) = 0, \tag{16}$$

$$N\left(U\frac{\partial U}{\partial X} + W\frac{\partial U}{\partial Z}\right) + LW(WX - UZ) + V\frac{\partial U}{\partial Y} = \tilde{\beta}_1 + \nu\frac{\partial^2 U}{\partial Y^2}, \tag{17}$$

$$N\left(U\frac{\partial W}{\partial X} + W\frac{\partial W}{\partial Z}\right) - LU(WX - UZ) + V\frac{\partial W}{\partial Y} = \tilde{\beta}_2 + \nu\frac{\partial^2 W}{\partial Y^2}. \tag{18}$$

Here $\tilde{\beta}_1$ and $\tilde{\beta}_2$ are pressure-gradient parameters defined by

$$\tilde{\beta}_1 = N\left(U_e\frac{\partial U_e}{\partial X} + W_e\frac{\partial U_e}{\partial Z}\right) + LW_e(W_eX - U_eZ), \tag{19a}$$

$$\tilde{\beta}_2 = N\left(U_e\frac{\partial W_e}{\partial X} + W_e\frac{\partial W_e}{\partial Z}\right) - LU_e(W_eX - U_eZ); \tag{19b}$$

the function S is obtained by integrating the expression

$$\frac{dS}{S} = \frac{[1 + \xi^2(t^2 - 1)]^{\frac{1}{2}}}{t(1 - \xi^2)}\,d\xi = \frac{h_1\,dx}{h_2} \tag{20}$$

subject to $S = 0$ at $\xi = -1$; and

$$N = \frac{St^2}{h_2}, \quad L = \frac{t^2}{S}\left(\frac{1}{h_2} + K_2\right). \tag{21}$$

Along the line of symmetry, equations (16) to (18) become:

$$N\left(\frac{\partial U}{\partial X} + W_Z\right) + \frac{\partial V}{\partial Y} - LUX = 0, \tag{22}$$

$$NU\frac{\partial U}{\partial X}+V\frac{\partial U}{\partial Y}=\beta_1^*+\nu\frac{\partial^2 U}{\partial Y^2}, \tag{23}$$

and

$$N\left(U\frac{\partial W_Z}{\partial X}+W_Z^2\right)-LU(W_Z X-U)+V\frac{\partial W_Z}{\partial Y}=\beta_2^*+\nu\frac{\partial^2 W_Z}{\partial Y^2}, \tag{24}$$

where W_Z denotes $\partial W/\partial Z$ and the pressure-gradient parameters β_1^* and β_2^* are now

$$\beta_1^*=NU_e\frac{\partial U_e}{\partial X},\quad \beta_2^*=N\left(U_e\frac{\partial W_{Ze}}{\partial X}+W_{Ze}^2\right)-LU_e(W_{Ze}X-U_e). \tag{25}$$

The appropriate boundary conditions are:

$$\left.\begin{aligned} &Y=0,\quad U=V=W_Z=0;\\ &Y\to\infty,\quad U\to U_e(X),\quad W_Z\to W_{Ze}(X).\end{aligned}\right\} \tag{26}$$

At the *stagnation point*, S_0, where both U and W are zero, the governing equations (22) to (24) and their boundary conditions (26) reduce to:

$$N(U_X+W_Z)+V_Y=0, \tag{27}$$

$$NU_X^2+V\frac{\partial U_X}{\partial Y}=\beta_1^{**}+\nu\frac{\partial^2 U_X}{\partial Y^2}, \tag{28}$$

$$NW_Z^2+V\frac{\partial W_Z}{\partial Y}=\beta_2^{**}+\nu\frac{\partial^2 W_Z}{\partial Y^2}; \tag{29}$$

$$\left.\begin{aligned} &Y=0,\quad U_X=V=W_Z=0;\\ &Y\to\infty,\quad U_X\to U_{Xe},\quad W_Z\to W_{Ze}.\end{aligned}\right\} \tag{30}$$

In equations (28) and (29), the pressure gradient parameters β_1^{**} and β_2^{**} are

$$\beta_1^{**}=NU_{Xe}^2,\quad \beta_2^{**}=NW_{Ze}^2. \tag{31}$$

2.3. *Line of symmetry transformations*

To solve the line of symmetry equations, we find it convenient to use a transformation which we employed in our previous studies (Hirsh & Cebeci 1977). For the nose-region equations given by (22), (23), (24) and (26), we let

$$\eta^*=\left(\frac{U_{\text{ref}}}{\nu c}\right)^{\frac{1}{2}}Y \tag{32}$$

and introduce a two-component vector potential (ϕ,ψ) such that

$$U=\frac{\partial\psi}{\partial Y},\quad W_Z=\frac{\partial\phi}{\partial Y},\quad V=-\left(N\frac{\partial\psi}{\partial X}+N\phi-L\psi X\right). \tag{33}$$

In addition, we define dimensionless functions F and G by

$$\psi=(U_{\text{ref}}\nu c)^{\frac{1}{2}}F(X,\eta^*),\quad \phi=(U_{\text{ref}}\nu c)^{\frac{1}{2}}G(X,\eta^*), \tag{34}$$

where U_{ref} and c are respectively a reference velocity and length introduced for convenience of comparison with Hirsh & Cebeci (1977); both are unity throughout this paper. The line of symmetry equations for the nose region may now be written as

$$F''' + F''(NG - LFX) = N\left(F'\frac{\partial F'}{\partial X} - F''\frac{\partial F}{\partial X}\right) - \beta_1^*, \tag{35}$$

$$G''' - N(G')^2 + LF'(G'X - F') + G''(NG - LFX) = N\left(F'\frac{\partial G'}{\partial X} - G''\frac{\partial F}{\partial X}\right) - \beta_2^*, \tag{36}$$

where primes denote differentiation with respect to η^* and

$$F' = \frac{U}{U_{\text{ref}}}, \quad G' = \frac{W_Z}{U_{\text{ref}}}. \tag{37}$$

The boundary conditions (26) become

$$\eta^* = 0, \quad F = F' = G = G' = 0;$$

$$\eta^* \to \infty, \quad F' \to \frac{U_e}{U_{\text{ref}}}, \quad G' = \frac{W_Z}{U_{\text{ref}}}. \tag{38}$$

3. Formulation for slender prolate spheroids

As we shall see later, it is desirable and convenient to study the boundary layers on very slender prolate spheroids, i.e. $t \to 0$. To obtain the governing equations appropriate for such bodies, we use the co-ordinates (14) and (15) and define

$$p = \frac{(1-\xi^2)^{\frac{1}{2}}}{t}. \tag{39}$$

Then we take the limit $t \to 0$, holding p and S finite. After some algebra, we obtain the following equations:

$$N\left(\frac{\partial U}{\partial X} + \frac{\partial W}{\partial Z}\right) + \frac{\partial V}{\partial Y} - L(UX + WZ) = 0, \tag{40}$$

$$N\left(U\frac{\partial U}{\partial X} + W\frac{\partial U}{\partial Z}\right) + V\frac{\partial U}{\partial Y} + LW(WX - UZ) = \tilde{\beta}_1 + \nu\frac{\partial^2 U}{\partial Y^2}, \tag{41}$$

$$N\left(U\frac{\partial W}{\partial X} + W\frac{\partial W}{\partial Z}\right) + V\frac{\partial W}{\partial Y} - LU(WX - UZ) = \tilde{\beta}_2 + \nu\frac{\partial^2 W}{\partial Y^2}. \tag{42}$$

Here

$$S = \frac{p}{(1+p^2)^{\frac{1}{2}} + 1}\exp\left[(1+p^2)^{\frac{1}{2}} - 1\right], \tag{43a}$$

$$N = \frac{S}{p}, \quad L = \frac{(1+p^2)^{\frac{1}{2}} - 1}{pS(1+p^2)^{\frac{1}{2}}}, \tag{43b}$$

$$\tilde{\beta}_1 = N\left(U_e\frac{\partial U_e}{\partial X} + W_e\frac{\partial U_e}{\partial Z}\right) + LW_e(W_eX - U_eZ), \tag{43c}$$

$$\tilde{\beta}_2 = N\left(U_e\frac{\partial W_e}{\partial X} + W_e\frac{\partial W_e}{\partial Z}\right) - LU_e(W_eX - U_eZ), \tag{43d}$$

and U_e is the limit of $u_e\cos\theta - w_e\sin\theta$ as $t \to 0$, i.e.

$$U_e = \frac{pX\cos\alpha}{S(1+p^2)^{\frac{1}{2}}} - 2\left(1 - \frac{pX^2L}{S}\right)\sin\alpha. \tag{43e}$$

Similarly,

$$W_e = \frac{pZ\cos\alpha}{S(1+p^2)^{\frac{1}{2}}} + \frac{2XZLp}{S}\sin\alpha. \tag{43f}$$

The boundary conditions satisfied by U, W, V are:

$$\left.\begin{aligned} &Y = 0, \quad U = V = W = 0; \\ &Y \to \infty, \quad U \to U_e, \quad W \to W_e. \end{aligned}\right\} \tag{44}$$

These equations are explicitly independent of t and moreover are free of singularities at $p = 0$. It can be expected therefore that the solution is also quite smooth and in particular at the nose, now defined by $X = Z = 0$, the numerical integration presents no difficulties. It is interesting to note from (43a) that a finite value of S corresponds to a finite value of p, with $S/p \to 1$ as $p \to 0$, and hence from (39) to a distance from the nose $O(t^2)$. The set of equations (40), (41), (42) is appropriate therefore within a distance from the nose of general axisymmetric thin smooth bodies of the order of the radius of curvature there.

To obtain the line of symmetry equations for the system given by (40) through (42) and (44), we define

$$\left.\begin{aligned} U &= U_0(X, Y) + O(Z^2), \quad V = V_0(X, Y) + O(Z^2), \\ W &= Z\exp\left[1-(1+p^2)^{\frac{1}{2}}\right] W_1(X, Y) + O(Z^3). \end{aligned}\right\} \tag{45}$$

We allow for negative values of X by permitting p to take negative values. When $p < 0$, the sign of S in (43a) must be changed and generally $x = S\,\mathrm{sgn}\,p$ in the limit $Z \to 0$. Near the line of symmetry the longitudinal and transverse components of velocity in the boundary layer are

$$\left.\begin{aligned} U &= U_0\,\mathrm{sgn}\,p + O(Z^2), \\ W &= \frac{Z}{S}\left(\frac{pW_1}{1+(1+p^2)^{\frac{1}{2}}} - U_0\right) + O(Z^3), \end{aligned}\right\} \tag{46}$$

and

respectively. We now substitute (45) into (40) to (42) and take the limit $Z \to 0$, obtaining the equations

$$\frac{\partial U_0}{\partial p} + \frac{(1+p^2)^{\frac{1}{2}}}{(1+p^2)^{\frac{1}{2}}+1} W_1 + (1+p^2)^{\frac{1}{2}} \frac{\partial V_0}{\partial Y} - \left(\frac{p}{(p^2+1)^{\frac{1}{2}}+1}\right) U_0 = 0, \tag{47}$$

$$\frac{U_0}{(1+p^2)^{\frac{1}{2}}} \frac{\partial U_0}{\partial p} + V_0 \frac{\partial U_0}{\partial Y} = \beta_1^* + \nu \frac{\partial^2 U_0}{\partial Y^2}, \tag{48}$$

$$\frac{U_0}{(1+p^2)^{\frac{1}{2}}} \frac{\partial W_1}{\partial p} + V_0 \frac{\partial W_1}{\partial Y} + \frac{U_0^2}{(1+p^2)^{\frac{1}{2}}} + \frac{W_1^2}{1+(1+p^2)^{\frac{1}{2}}} - \Lambda_0 U_0 W_1 = \beta_2^* + \nu \frac{\partial^2 W_1}{\partial Y^2}, \tag{49}$$

with boundary conditions

$$\left.\begin{aligned} &Y = 0, \quad U_0 = V_0 = W_1 = 0; \\ &Y \to \infty, \quad U_0 \to U_{0e}, \quad W_1 \to W_{1e}. \end{aligned}\right\} \tag{50}$$

Here

$$\left.\begin{aligned}\beta_1^* &= \frac{U_{0e}}{(1+p^2)^{\frac{1}{2}}}\frac{U_{0e}}{p}, \quad \Lambda_0 = \frac{p}{1+p^2}+\frac{p}{1+p^2+(1+p^2)^{\frac{1}{2}}},\\ \beta_2^* &= \frac{U_{0e}}{(1+p^2)^{\frac{1}{2}}}\frac{\partial W_{1e}}{\partial p}+\frac{U_{0e}^2}{(1+p^2)^{\frac{1}{2}}}-U_{0e}W_{1e}\Lambda_0+\frac{W_{1e}^2}{1+(1+p^2)^{\frac{1}{2}}},\end{aligned}\right\} \tag{51}$$

and

$$\left.\begin{aligned}U_{0e} &= \frac{p\cos\alpha-2\sin\alpha}{(1+p^2)^{\frac{1}{2}}},\\ W_{1e} &= \frac{[(1+p^2)^{\frac{1}{2}}+1]\cos\alpha+2p\sin\alpha}{(1+p^2)^{\frac{1}{2}}}.\end{aligned}\right\} \tag{52}$$

In order to put the above equations into a more convenient form (see § 4), we now define η and $\overline{V}$ by

$$\eta = \frac{Y}{(1+p^2)^{\frac{1}{4}}}\frac{1}{\nu^{\frac{1}{2}}}, \quad \overline{V} = V_0\frac{(1+p^2)^{\frac{1}{4}}}{\nu^{\frac{1}{2}}}-\frac{\eta p U_0}{2(1+p^2)}, \tag{53}$$

and write the continuity equation (47) and the two momentum equations (48) and (49) as

$$\frac{\partial U_0}{\partial p}+\frac{\partial \overline{V}}{\partial \eta}+a_1U_0+a_2W_1 = 0, \tag{54}$$

$$U_0\frac{\partial U_0}{\partial p}+\overline{V}\frac{\partial U_0}{\partial \eta} = \beta_1^*+\frac{\partial^2 U_0}{\partial \eta^2}, \tag{55}$$

$$U_0\frac{\partial W_1}{\partial p}-a_3U_0W_1+a_2W_1^2+U_0^2+\overline{V}\frac{\partial W_1}{\partial \eta} = \beta_2^*+\frac{\partial^2 W_1}{\partial \eta^2}. \tag{56}$$

Here a_1, a_2 and a_3 are functions of p and are given by

$$\left.\begin{aligned}a_1 &= \frac{p}{2(1+p^2)}-\frac{p}{(p^2+1)^{\frac{1}{2}}+1}, \quad a_2 = \frac{(1+p^2)^{\frac{1}{2}}}{(1+p^2)^{\frac{1}{2}}+1},\\ a_3 &= \frac{p}{(1+p^2)^{\frac{1}{2}}}+\frac{p}{(1+p^2)^{\frac{1}{2}}+1}.\end{aligned}\right\} \tag{57}$$

The pressure-gradient parameters on (55) and (56) are

$$\beta_1^* = U_{0e}\frac{\partial U_{0e}}{\partial p}, \quad \beta_2^* = U_{0e}^2-a_3U_{0e}W_{1e}+U_{0e}\frac{\partial W_{1e}}{\partial p}+a_2W_{1e}^2, \tag{58}$$

and the boundary conditions (50) remain unaffected, except that now Y is replaced by η. At the stagnation point, (54), (55) and (56) become

$$U_1+\frac{\partial \overline{V}}{\partial \eta}+a_2W_1 = 0, \tag{59}$$

$$U_1^2+\overline{V}\frac{\partial U_1}{\partial \eta} = \beta_1+\nu\frac{\partial^2 U_1}{\partial \eta^2} \tag{60}$$

and

$$a_2W_1^2+\overline{V}\frac{\partial W_1}{\partial \eta} = \beta_2+\nu\frac{\partial^2 W_1}{\partial \eta^2}, \tag{61}$$

where $U_1 = \partial U_0/\partial p$;

$$\eta = 0, \quad U_1 = \bar{V} = 0, \quad W_1 = 0, \quad \eta \to \infty, \quad U_1 \to U_{0e}, \quad W \to W_{1e}. \tag{62}$$

The pressure gradient parameters $\tilde{\beta}_1$ and $\tilde{\beta}_2$ are

$$\tilde{\beta}_1 = U_{1e}^2, \quad \tilde{\beta}_2 = a_2 W_{1e}^2, \tag{63}$$

and

$$U_{1e} = \frac{\cos\alpha}{(1+p_0^2)^{\frac{1}{2}}}, \quad W_{1e} = \frac{[(p_0^2+1)^{\frac{1}{2}}+1]\cos\alpha + 2p_0\sin\alpha}{(p_0^2+1)^{\frac{1}{2}}}, \tag{64}$$

with

$$p_0 = 2\tan\alpha. \tag{65}$$

4. Results

In this paper we concentrate on the solution of the line-of-symmetry equations for the cases of finite thickness and 'zero' thickness and as a function of the angle of attack using the numerical method described in Cebeci & Bradshaw (1977). The solution of the equations off the line of symmetry for both cases is still in progress and will be reported later.†

4.1. *Asymptotic theory for zero-thickness case*

It is appropriate to consider some general properties of the solution before the presentation of the numerical results for the line-of-symmetry equations for the zero-thickness case. The solution starts at the stagnation point where we solve the equations given by (59) to (62) and the solution is an example of the stagnation flow studied by Howarth (see Brown & Stewartson 1969). On the windward side, p increases and the solution of (54) to (56) can be expected to approach a simple asymptotic form as $p \to \infty$. Now as $p \to \infty$, i.e. far from the nose on the windward side, it is consistent to assume that all dependent variables become independent of p and we have, with

$$\bar{V} = -\Psi_0(\eta), \quad W_1 - U_0 = \Psi_0'(\eta), \tag{66}$$

and primes denoting differentiation with respect to η,

$$U_0'' + \Psi_0 U_0' = 0, \tag{67}$$

$$\Psi_0''' + \Psi_0\Psi_0'' - (\Psi_0')^2 + (2\sin\alpha)^2 = 0, \tag{68}$$

where

$$\Psi_0(0) = \Psi_0'(0) = U_0(0) = 0 \tag{69a}$$

and

$$\Psi_0'(\infty) = 2\sin\alpha, \quad U_0(\infty) = \cos\alpha. \tag{69b}$$

Thus the asymptotic solution on the windward side is essentially the same as that for a forward stagnation point in two dimensions together with a transverse boundary layer due to a uniform 'crossflow'. The roles of crossflow and mainstream seem in fact to be reversed for our problem: W is the crossflow and is proportional to Ψ_0' when $p \gg 1$ [see equation (46)]. Suitable properties of the asymptotic solution which may be compared with numerical results include

$$U_0'(0) \to 0{\cdot}5788(2\sin\alpha)^{\frac{1}{2}}\cos\alpha, \tag{70}$$

† A preliminary account of this work is given in Cebeci, Khattab & Stewartson (1979).

$$W_1'(0) \to 1{\cdot}2326(2\sin\alpha)^{\frac{3}{2}} + 0{\cdot}5788\cos\alpha(2\sin\alpha)^{\frac{1}{2}}, \tag{71}$$

$$\Delta_1 = \int_0^\infty (U_e - U_0)\, d\eta \to 1{\cdot}016(2\sin\alpha)^{\frac{1}{2}}\cos\alpha, \tag{72}$$

$$\Delta_2 = \int_0^\infty (W_e - W_1)\, d\eta \to \Delta_1 + 0{\cdot}6479(2\sin\alpha)^{\frac{1}{2}} \tag{73}$$

as $p \to \infty$.

On the leeward side, we integrate in the direction of p decreasing and once we are past the nose, so that p is negative, either $\partial U/\partial\eta$ vanishes at some finite value $p_s(\alpha)$ of p or it reaches a (negative) maximum (see figure 5) then decreases again. In the first case a singularity develops at $p = p_s$ (see Brown & Stewartson 1969) and in the second the solution can be continued to all negative values of p and there is a consistent asymptotic form which it approaches as $p \to -\infty$. This form is in two parts. Near the body ($\eta \sim 1$) we write, for large negative values of p,

$$\overline{V} = -\Phi_0(\eta), \quad W_1 + U_0 = \Phi_0'(\eta), \tag{74}$$

so that from (46) $-\phi_0'$ gives the cross-flow velocity W. Then ϕ_0 satisfies the same differential equations as Ψ_0, and U_0 satisfies (67) and (68). The boundary conditions are also the same as (69) but some comment is needed about $\phi_0'(\infty)$. According to (52) $\phi_0'(\infty)$ should be equal to $-2\sin\alpha$ but it is well known that (67) and (68) do not then have a solution. The solution of this apparent contradiction is to be found in Proudman & Johnson's study of the unsteady boundary layer near the rear stagnation point of a two-dimensional bluff body (Proudman & Johnson 1962). This asymptotic solution may easily be adapted to our problem with p playing the role of time. The appropriate boundary condition to complete the specification of (75), (77) is then

$$\Phi_0'(\infty) = +2\sin\alpha \tag{75}$$

which means that near the body $W/\cos\theta > 0$ and so the boundary layer behaves on the leeside and windward sides in essentially the same way – fluid is being carried along the line of symmetry and nearby the streamlines are curved away from it so that fluid is also moving out of the symmetry plane. Also apart from the obvious change in sign of $U_0'(0)$, the properties (70) and (73) are the same on the leeward side.

As $\eta \to \infty$, $U_0 \to -\cos\alpha$ and $W_1 + U_0 \to 2\sin\alpha$ whereas it should be $\to -2\sin\alpha$. The adjustment of this boundary condition takes place over a length scale in η which is an exponentially large function of p and in which viscous forces can be neglected and U_0 may be regarded as sensibly constant. We write

$$\xi = \eta\exp(2p\tan\alpha), \tag{76}$$

$$\overline{V} = 2\sin\alpha\, e^{-2p\tan\alpha} F(\xi), \quad W_1 + U_0 = -2\sin\alpha F'(\xi), \tag{77}$$

where primes now denote differentiation with respect to ξ. On substituting into (54), (56) we obtain

$$(F - \xi)F'' = F'^2 - 1 \tag{78}$$

with boundary conditions

$$F' \to 1 \quad \text{as} \quad \xi \to \infty, \quad F(0) = 0, \tag{79}$$

to match up with the prescribed mainstream conditions and with the inner solution

(74) valid when $n \sim 1$ and hence when $\xi \ll 1$. Specifically we notice that $F(0) = 0$ implies $F'(0) = -1$. The solution of (78) is

$$F = \xi - \frac{2}{c}(1 - e^{-\xi c}), \tag{80}$$

where c is a constant dependent in some way on the history of the boundary layer for finite p and determined by matching with the numerical computation. Reference may be made to Proudman & Johnson's paper for details of the arguments leading to the choice of the scaling law (78) and discussion of various alternatives.

A possible interpretation of this result is as follows. There is a curve C on the paraboloid, symmetric with respect to the leeward line of symmetry l and open as $p \to -\infty$ on which the crossflow skin friction is zero. The limiting streamlines (or skin-friction lines) of the boundary layer all start from the stagnation point S_0 and two of them are the windward l_w and leeward l lines of symmetry. Limiting streamlines initially inclined close to l_w move away from it as S increases ultimately asymptoting to C when $\theta \simeq 105°$ (see Cebeci & Bradshaw 1977) corresponding to the separation angle for a circular cylinder. The other limiting streamlines also move away from l_w and, once the nose is passed, towards l, but eventually they must cross C when they turn back towards l_w, but never reaching it of course. Instead they either asymptote to C from the other side as $p \to -\infty$ or generate a separation line at finite values of p.

A surface Σ can also be defined, standing on C, on which the cross velocity is zero. One of its principal properties is that its height increases exponentially as $p \to -\infty$. Streamlines in the boundary layer initially above the limiting streamlines in the neighbourhood of l_w are directed away from the paraboloid and this line and pass above Σ. Other streamlines also move initially towards l and away from the body but once they cross Σ the crossflow velocity is reversed and they begin to move back towards l_w. Further if they are sufficiently near the body their outward motion is temporarily also reversed, but not at Σ. Eventually they will again move away from the body and are likely to end up asymptoting the inside of Σ or some separation surface. Thus, the general shape of the streamlines is spiral although it is unlikely that more than one revolution is completed. Complications would arise if the streamlines formed internal envelopes but evidence is lacking in support of these possibilities.

4.2. *The two-dimensional airfoil*

The equivalent results for the boundary layer near the nose of a two-dimensional bluff body are obtained in a more straightforward way than for bodies of revolution, but the fundamental equations take a little more space to derive because a suitable reference is lacking. We begin by considering the inviscid flow past an ellipse at an incidence α with circulation $2\pi\kappa$ (neglected in § 2). We define (x, y) as Cartesian co-ordinates with origin O at the centre of the ellipse Ox along the major axis and Oy along the minor axis. Then, according to complex variable theory, the complex potential for attached flow is

$$w = \zeta e^{-i\alpha} + \zeta^{-1} e^{i\alpha} + i\kappa \log \zeta, \quad z = \zeta + c^2/\zeta, \tag{81}$$

where $w = \phi + i\psi$, ψ is the stream function of the flow and $z = x + iy$. In this solution the circle $\zeta = -e^{-i\theta}$ corresponds to the ellipse $x = -(1 + c^2)\cos\theta$, $y = (1 - c^2)\sin\theta$ and

non-dimensional variables are used so that the fluid speed at infinity is unity and the major axis of the ellipse is $2(1+c^2)$.

We are specifically interested in the neighbourhood of the nose (i.e. $x = -(1+c^2)$, $y = 0$) when $0 < (1-c^2) \ll 1$. Let us write $1-c^2 = 2t$, so that t is the (small) thickness ratio of the ellipse and

$$\theta = -t\xi. \tag{82}$$

On the ellipse and near the nose $x+2 = t^2\xi^2$, $y = 2t^2\xi$, and the velocity of slip round the ellipse is

$$u_e(\xi) = \frac{\xi-\beta}{(\xi^2+1)^{\frac{1}{2}}}, \tag{83}$$

when $\xi = O(1)$, where $\beta t = (2\alpha-\kappa)$. From thin airfoil theory we may take $\kappa = \alpha$ and we shall assume $\beta > 0$.

The boundary-layer equations needed to reduce this slip velocity to zero at the ellipse are now easily obtained. We suppose, that the normal distance Y from the ellipse and the stream function ψ are scaled with $t(2\nu)^{\frac{1}{2}}$ where ν is the kinematic viscosity and arc length X on the ellipse with $2t^2$ so that

$$X = \tfrac{1}{2}\xi(1+\xi^2)^{\frac{1}{2}} + \tfrac{1}{2}\sinh^{-1}\xi. \tag{84}$$

With external velocity distribution given by (83) and with surface distance given by (84), the governing boundary-layer equations are solved by the Box scheme described in Cebeci & Bradshaw (1977). The solution procedure starts at $\bar{X} = 0$ with $\xi = \beta$ where

$$\bar{X} = X - X_0,$$

with X_0 computed from (84) by letting $\xi = \beta$. The integration, which starts as the Hiemenz stagnation point flow, tends to the Blasius form on the pressure side of the airfoil as $X \to +\infty$. On the suction side X decreases and u_e reaches a negative minimum value of $-(1+\beta^2)$ at $\xi = -1/\beta$, i.e. just past the nose, and thereafter increases again to -1 as $X \to -\infty$ (see figure 2). Provided, therefore, that the integration does not breakdown at a finite value of X, the solution on the suction side also takes on the Blasius form as $X \to -\infty$. However, if the pressure gradient parameter β is strong enough, the solutions predict separation, where they break down. The condition is

$$\beta > \beta^* = 1{\cdot}155. \tag{85}$$

For such values of β, the solution is terminated at the separation point $\bar{X}_s$ shown in figure 3 as a function of β. It is interesting to compare this criterion for the onset of separation with the experimental data provided by Gault (1955). For the N.A.C.A. 663–018 airfoil with a leading-edge radius of curvature corresponding to $t = 0{\cdot}20$, he found that incipient separation occurs when $\alpha = 7°$, i.e. $\beta = 0{\cdot}61$. The most likely explanation for the discrepancy with (85) is that this airfoil is not exactly parabolic near the nose. Thus, if we define β by the position of the forward stagnation point, $\beta = 1$ at $\alpha = 7°$ and if we define it by the pressure minimum $\beta = 1{\cdot}45$. A somewhat similar situation occurs with the modified N.A.C.A. 0010 airfoil. Here $t = 0{\cdot}16$ and the corresponding values of β are 0·43, 0·6 and 1·0.

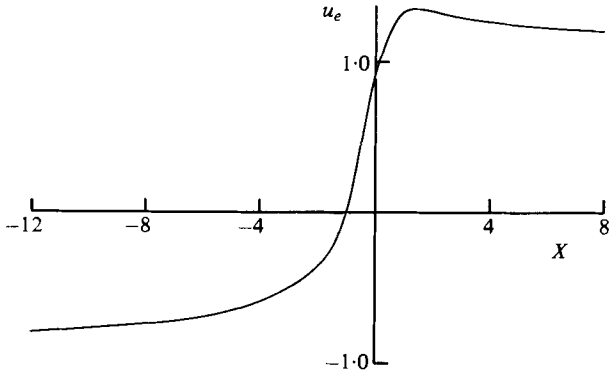

FIGURE 2. Variation of u_e with X for $\beta = 0{\cdot}9$.

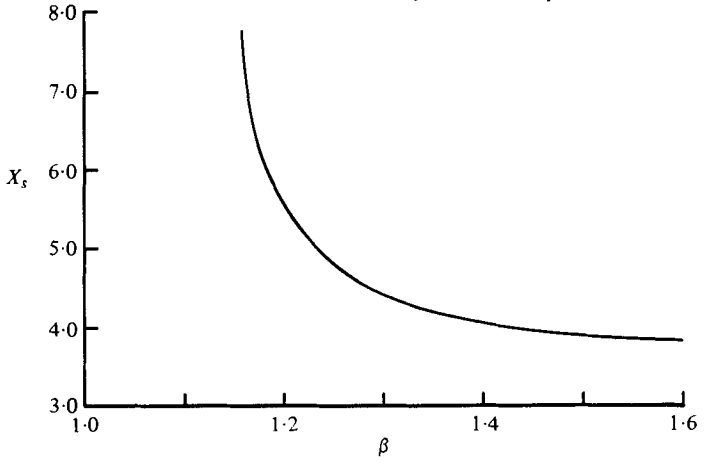

FIGURE 3. Variation of separation point with β.

4.3. *Numerical results for the line-of-symmetry flow*

The numerical results obtained here are in quite good agreement with the earlier results for finite thickness by Wang (1970) and by Hirsh & Cebeci (1977) and for 'zero'-thickness by the asymptotic theory of § 4.1. For the zero-thickness case, which we consider first, figures 4 and 5 show the variation of the longitudinal and transverse components of wall shear, $U_0'(0)$ and $W_1'(0)$, with p for various values of α. On the leeward side the longitudinal component of the wall shear develops a maximum and a minimum at moderate, but not too large, values of α. As α increases, the peak and dip in the wall shear on the leeward side near the nose becomes more pronounced and at $\alpha = 41°$, this component of the wall shear actually vanishes at $p_s = -1{\cdot}38$, terminating the computation. At larger values of α, it vanishes nearer the nose and indeed formally we may expect that as $\alpha \to 90°$, separation takes place at $p = 0$. The variation of p_s with α is shown in figure 6. Also shown in figures 4 and 5 are the asymptotic values for $U_0'(0)$, $W_0'(0)$ and $\alpha = 30°$ both on the windward and leeward sides computed from (69) *et seq.* It is clear that the results are consistent.

The calculations for the leeward side also indicate that in the region where $U_0'(0)$ exhibits a maximum and a minimum, the boundary-layer thicknesses of U_0 and W_1 are nearly the same. After the dip in $U_0'(0)$ or rise in $W_0'(0)$ (see figure 5), the crossflow

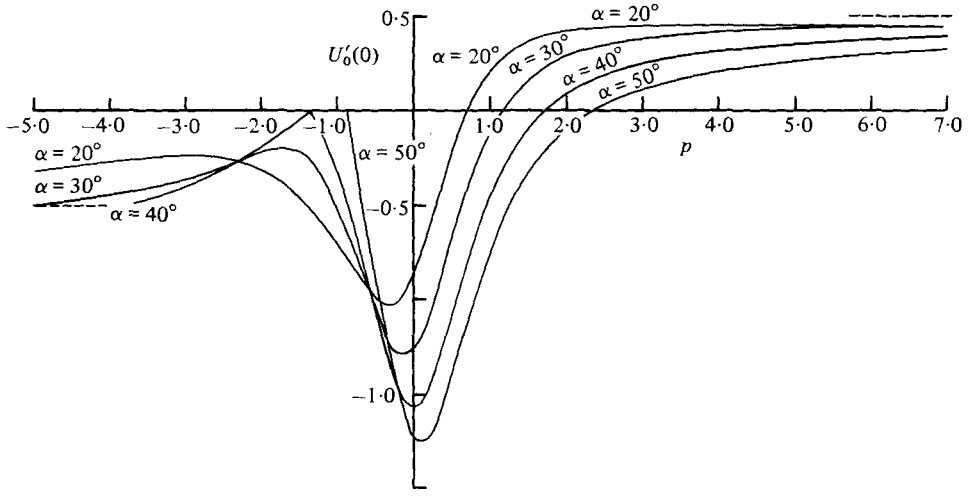

FIGURE 4. Variation of the longitudinal component of wall shear, $U_0'(0)$ for paraboloids of zero thickness ratio with p for various α. The dashed lines indicate the asymptotic results for $\alpha = 30°$.

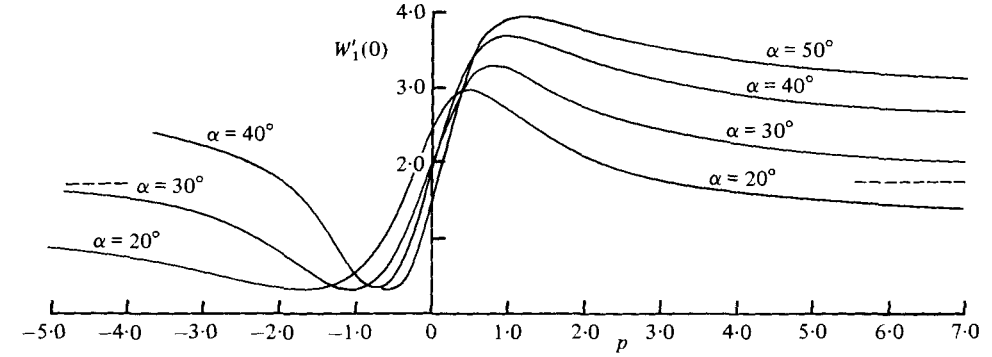

FIGURE 5. Variation of the transverse component of wall shear, $W_1'(0)$ for paraboloids of zero thickness ratio with p for various α. The dashed lines indicate the asymptotic results for $\alpha = 30°$.

component develops a very thick boundary layer while the boundary thickness of the longitudinal component of the flow remains nearly unchanged. Figure 7 shows the variation of the crossflow profile wS/Z [see equation (46)] on the leeward side for various values of p at $\alpha = 30°$. The double structure appears to be developing quite strongly with the inner part asymptoting to the limit (74); the outer part is thickening rapidly but p is too small for us to comment with definiteness on the relevance of (76), (80). In figure 8 we display the variation of the displacement thicknesses Δ_1, Δ_2 on the windward and leeward sides and compare with the asymptotic theory. The agreement is good and we note in particular that Δ_2 increases rapidly as p decreases below p_s.

For $t \neq 0$ the numerical procedure is to solve the transformed equations, (22)–(24), in the neighbourhood of the nose and then at a convenient station of X to switch back to the equations in terms of x and y, equations (10)–(12). The chief results are displayed in figure 9 which shows, for the finite-thickness case ($t = \frac{1}{4}$), the variation of the longitudinal local skin-friction coefficient, c_f, for various angles of incidence. These results agree quite well with those computed by Hirsh & Cebeci (1977) who

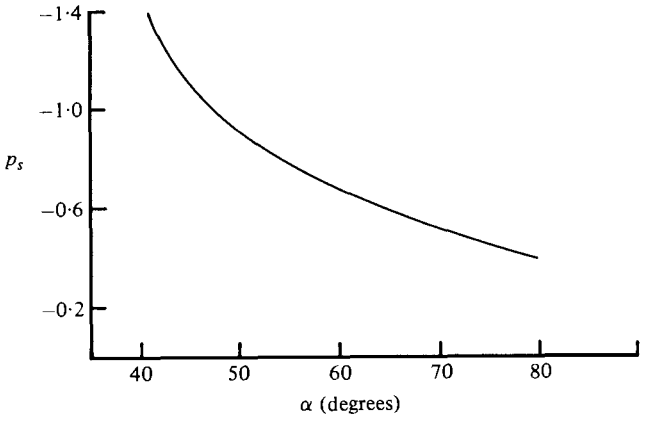

FIGURE 6. The variation of separation point p_s on paraboloids of zero thickness ratio with α.

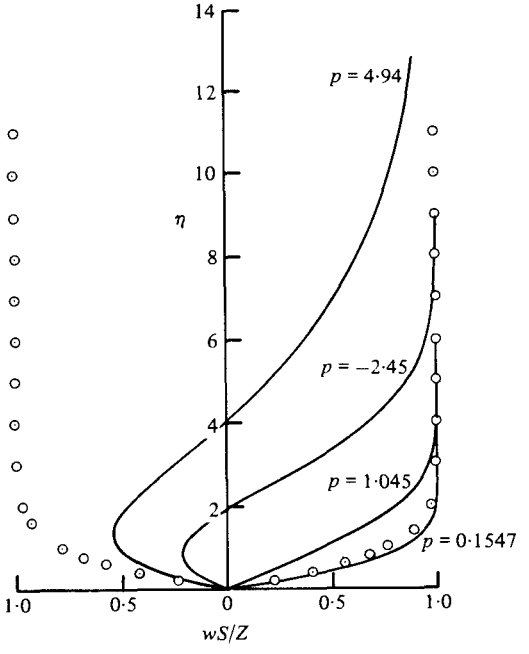

FIGURE 7. The profiles of the crossflow velocity w at $\alpha = 30°$ for various values of p: ⊙, the asymptotic forms, windward to the right and leeward to the left. The dependence of w on Z/S has been scaled out.

considered only small angles of incidence and with those of Wang (1970) who considered larger angles of incidence. The results also show, as in the zero-thickness case, that the peak and dip in the skin-friction coefficient on the leeward side near the nose becomes more pronounced with increasing angle of incidence and, the local skin-friction vanishes at approximately 42 degrees, indicating separation. It is remarkable that this result is in excellent agreement with the one computed by using the zero-thickness case. Further comparisons and calculations will be made when the solutions are extended off the line of symmetry for both zero- and finite-thickness cases.

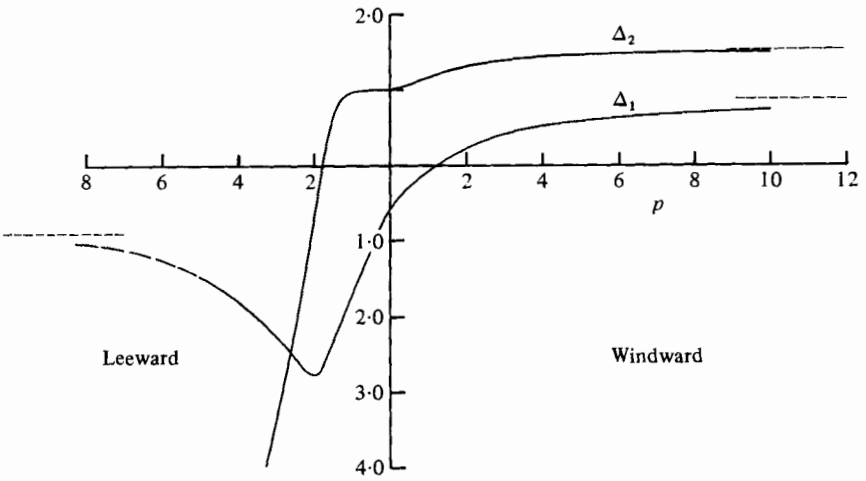

FIGURE 8. The variation of Δ_1, Δ_2 for paraboloids of zero thickness with p for $\alpha = 30°$. The dashed lines are the asymptotic results.

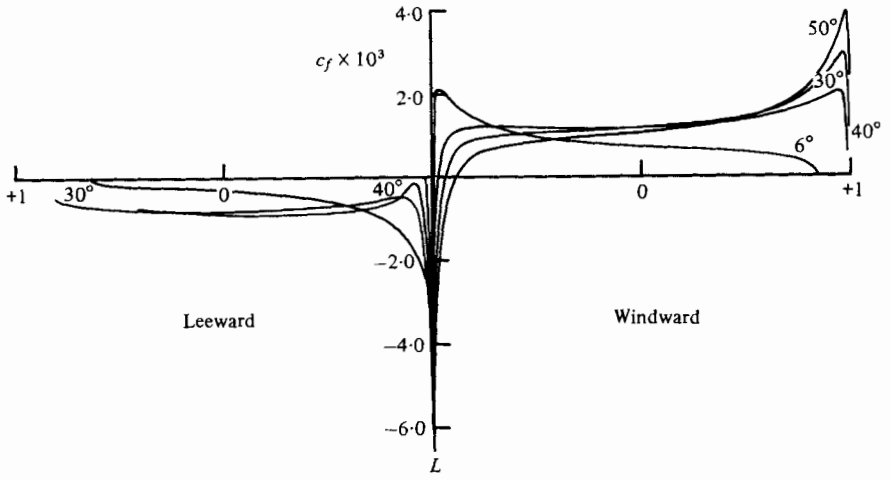

FIGURE 9. The variation of the longitudinal local skin-friction coefficient, c_f, with axial distance from the nose ($x = -1$) for a spheroid of thickness ratio $\frac{1}{4}$ and various angles of incidence.

5. Discussion

The principal result of this study is to bring out the difference between the phenomenon of nose-separation on thin two-dimensional and axisymmetric bodies set at an angle α to the oncoming flow. For two-dimensional bodies, or airfoils, it first occurs at $\alpha \simeq 1{\cdot}155$ where t is a representative thickness parameter of the body but for axisymmetrical bodies it is delayed until $\alpha \simeq 41°$ no matter how small t is. Indeed from the earlier results at finite values of t, due to Wang (1974) we might expect that nose-separation cannot occur if $\alpha < 41°$ for all prolate spheroids. Care must, of course, be taken in interpreting these contrasting conclusions. In two-dimensional flows we are essentially only concerned with separation points and nothing can be said in the present context about the flow in the boundary layer further downstream in view of

FIGURE 10. Sketch of open separation.

the singularity in the solution at separation. However, in three-dimensional boundary-layer studies we must consider separation lines and we have only established the likelihood of these lines intersecting the leeward line of symmetry l when $\alpha > 41°$. For α close to but less than 41°, the separation lines may extend to points near the nose without reaching as far as l. Thus Wang (1974) finds that when $\alpha = 30°$, $t = \frac{1}{4}$ the separation line extends as near as $\xi \simeq -0{\cdot}9$ to the nose. He concludes that a new phenomenon occurs, which he terms 'open separation' having the property that the separation line is an envelope of limiting streamlines on both sides (figure 10). Now separation on l occurs at $\xi \simeq +0{\cdot}9$ but he was only able to compute a very small part of the flow field on the leeward side of this separation line. It is possible that as $\alpha \rightarrow \alpha_s(t)$, where $\alpha_s(t)$ is the minimum angle of attack provoking nose-separation on l, the upstream end of his open separation line moves up to l and for $\alpha > \alpha_s$ the separation line is closed once more. Further study of the region between the open separation line and l is clearly needed and the extension of the present theory to points off l may be the simplest way of dealing with it, since the governing equations are now free of irregularities and any small quantities have been rendered innocuous.

The results obtained so far also raise some interesting questions when $t \ll 1$. For in the limit $t \rightarrow 0$ one can interpret the main stream flow at large values of p as consisting of two components, of which the one in the cross-plane of the body corresponds to the flow of a fluid past a circular cylinder of very slowly varying radius and uniform at large distances from it. The other component is uniform and directed along the normals to this cross-plane. The situation is very like that for a yawed infinite wing in fact. The associated boundary layers on the line of symmetry have an asymptotic structure which supports this view and are consistent with their numerical solution at finite p. Hence in view of the independence principle for yawed infinite wings (Jones 1947) we should be able to integrate the crossflow equations (for w) independently of that for u when $p \gg 1$ and since these lead to separation at $\theta \simeq 105°$ (Cebeci & Bradshaw 1977) this line should be the asymptote of Wang's open separation line when $\alpha < \alpha_s(0)$ and $|p| \rightarrow \infty$.

However, we are inclined to be cautious at present. For the singularity in the crossflow boundary layer at separation prevents the above asymptotic solution from being continued to larger values of θ whereas we know from the leeward line of symmetry solution that one can be found at $\theta = \pi$ for all p. Further the use made of the Proudman–Johnson theory in §4.1 suggests that there is an analogy between the role of p in the present theory and of τ, the time, in unsteady two-dimensional theory. There has been some controversy in the past about the properties of unsteady boundary layers on circular cylinders, particularly as to whether they can develop singularities at finite times. The present position is that they remain smooth for $\tau < 1{\cdot}4$ (e.g. Cebeci 1979) although growing rapidly downstream of separation, exponentially so

near the rear-stagnation point. Cebeci argues, and we concur, that the solution is free of singularities for all time (but see Wang 1979).

The main differences between unsteady boundary layers and steady boundary layers with $t = 0$ occur near the body, when $\eta \sim 1$ and u_0 is not sensibly constant so that the analogy fails, and near the nose ($p \sim 1$) when in addition separation occurs on l if $\alpha > \alpha_s(0)$. If we assume that the analogy qualitatively holds provided $\alpha < \alpha_s(0)$ we may infer that the flow is smooth over the nose region for all finite p but that beyond a certain line, roughly given by the reversal of the crossflow component of the skin friction the crossflow boundary-layer thickness rapidly increases in thickness with p. The failure of the analogy when $\eta \sim 1$ means that, not withstanding the claimed smoothness of the unsteady solution for all τ, there may still exist an open separation line or even a separation tongue with one or both ends asymptoting to $\theta \simeq 105°$ as $p^2 \to \infty$.

This discussion seems to have relevance to yawed wings which are not axisymmetric. The independence principle applies here too and would suggest that the boundary solution must be terminated at the separation of the crossflow. We now wonder whether this is necessarily the case. Provided separation of the boundary-layer component in the spanwise direction has not occurred near the upstream wing-tip and the distance from the tip is finite, it may be possible to carry out the integration beyond the crossflow reversal right up to the trailing edge. Of course, the crossflow boundary layer then increases in thickness rapidly with p but the boundary-layer assumptions are still valid so that we would be able, without any contradictions, to advance the integration beyond the separation line in the form it is understood at present. The avoidance of separation near the wing-tip might, however, not be easy in practice, especially since an unyawed wing corresponds essentially to setting $\alpha = 90°$.

A final question raised by these studies concerns the flow near the nose of smooth three-dimensional bodies, for example thin ellipsoids at incidence. If the mainstream is symmetric about a plane of symmetry of the ellipsoid, then the boundary layer on one of the lines of symmetry can be computed using similar methods to those of this report and indeed our present results can be regarded as limiting cases accordingly as the cross-section of the ellipsoid is a circle (§ 4.1) or has an infinite major axis (§ 4.2). Presumably the critical angle for nose separation varies from 41° to 0° as the eccentricity of the cross-section increases from 0 to 1. It would be interesting to know how close we must be to a two-dimensional form before separation occurs at relatively small angles of attack and indeed what is the effect of an asymmetric mainstream so that there is no line of symmetry along which the integration can be carried out independently of the rest of the flow field.

This work was supported by the Naval Surface Weapons Center under contract N60921-77-C-0096.

REFERENCES

Briley, W. R. & McDonald, H. 1955 Prediction of incompressible separation bubbles. *J. Fluid Mech.* **6**, 631–656.

Brown, S. N. & Stewartson, K. 1969 Laminar separation. *Ann. Rev. Fluid Mech.* **1**, 45–72.

Cebeci, T. 1979 The laminar boundary layer on a circular cylinder started impulsively from rest. *J. Comp. Phys.* **31**, 153–172.

CEBECI, T. & BRADSHAW, P. 1977 *Momentum Transfer in Boundary Layers.* McGraw-Hill and Hemisphere.

CEBECI, T., KAUPS, K., MOSINSKIS, G. J. & REHN, J. A. 1973 Some problems of the calculation of three-dimensional boundary-layer flows on general configurations. *N.A.S.A.* CR-2285.

CEBECI, T., KHATTAB, A. K. & STEWARTSON, K. 1979 Prediction of three-dimensional laminar and turbulent boundary layers on bodies of revolution at small angles of attack. *Proc. 2nd Symp. on Turbulent Shear Flows, London.*

GASTER, M. 1966 The structure and behavior of laminar separation bubbles. Separated flows. Part 2. *AGARD Conf. Proc.* no. **4**, 819.

GAULT, D. E. 1955 An experimental investigation of regions of separated laminar flow. *N.A.C.A. Tech. Note* 3505.

GEISSLER, W. 1974 Three-dimensional laminar boundary layer over a body of revolution at incidence and with separation. *A.I.A.A. J.* **12**, 1743–1745.

GOLDSTEIN, S. 1948 On laminar boundary-layer flow near a position of separation. *Quart. J. Mech. Appl. Math.* **1**, 43.

HIRSH, R. S. & CEBECI, T. 1977 Calculation of three-dimensional boundary layers with negative crossflow on bodies of revolution. *A.I.A.A. paper* 77-683.

JONES, B. M. 1934 Stalling. *J. Roy. Aero. Soc.* **38**, 753–770.

JONES, R. T. 1947 Effects of sweepback on boundary layer and separation. *N.A.C.A.* TR 884.

PROUDMAN, I. & JOHNSON, K. 1962 Boundary-layer growth near a rear stagnation point. *J. Fluid Mech.* **14**, 161–168.

SMITH, F. T. 1977 The laminar separation of an incompressible fluid streaming past a smooth surface. *Proc. Roy. Soc.* A **356**, 443–464.

SMITH, F. T. 1979 Laminar flow of an incompressible fluid past a bluff body; the separation, reattachment, eddy properties and diag. *J. Fluid Mech.* **92**, 171–205.

TANI, T. 1964 Low-speed flows involving bubble separations. *Prog. Aero. Sci.* **5**, 70–103.

WANG, K. C. 1970 Three-dimensional boundary layer near the plane of symmetry of a spheroid at incidence. *J. Fluid Mech.* **43**, 187–209.

WANG, K. C. 1974 Boundary layer over a blunt body at high incidence with an open-type of separation. *Proc. Roy. Soc.* A **340**, 33–55.

WANG, K. C. 1975 Boundary layer over a blunt body at low incidence with circumferential reversed flow. *J. Fluid Mech.* **72**, 49–65.

WANG, K. C. 1976 Separation of three-dimensional flow in reviews in viscous flows. *Proc. Lockheed-Georgia Co. Viscous Flow Symp.*, pp. 341–414.

WANG, K. C. 1979 Unsteady boundary-layer separation. *Martin Marietta Labs. Rep.* TR79-16c.